A Dorsal Visual Route Necessary for Global Form Perception: Evidence from Neuropsychological fMRI

Vaia Lestou[1], Judith Mi Lin Lam[2], Katie Humphreys[1], Zoe Kourtzi[1], and Glyn W. Humphreys[3]

Abstract

■ Hierarchical models of visual processing assume that global pattern recognition is contingent on the progressive integration of local elements across larger spatial regions, operating from early through intermediate to higher-level cortical regions. Here, we present results from neuropsychological fMRI that refute such models. We report two patients, one with lesions to intermediate ventral regions and the other with damage around the intraparietal sulcus (IPS). The patient with ventral damage showed normal behavioral and BOLD responses to global Glass patterns. The patient with IPS damage was impaired in discriminating global patterns and showed a lack of significant responses to these patterns in intermediate visual regions spared by the lesion. However, this patient did show BOLD activity to translational patterns, where local element relations are important. These results suggest that activation of intermediate ventral regions is not necessary to code global patterns; instead global patterns are coded in a heterarchical fashion. High-level regions of dorsal cortex are necessary to generate global pattern coding in intermediate ventral regions; in contrast, local integration processes are not sufficient. ■

INTRODUCTION

Visual object recognition is frequently attributed to a hierarchically arranged set of processes, in which global representations are formed by integrating local elements into global forms or extracting in parallel different spatial frequency components that characterize local and global elements. According to this local-to-global hierarchical view, local elements are first encoded by early visual areas (V1/V2) and then integrated within intermediate regions (V3/V4). The output of this integration process is then forwarded to higher-level regions responding to global pattern structure (e.g., the lateral occipital complex [LOC], more anterior temporal cortex). Consistent with this view, lesions to intermediate visual areas are associated with disorders in the organization of visual elements into recognizable whole patterns (Giersch, 2002; Milner et al., 1991; Riddoch & Humphreys, 1987).

In contrast to the view that recognition proceeds through hierarchical processing in the ventral visual stream, there is increasing evidence for the role of dorsal cortex in form processing. For example, Konen and Kastner (2008) have reported object-selective responses within both intermediate (V3a) and higher-level regions of the dorsal visual stream (e.g., the intraparietal sulcus [IPS]). Although these studies can be interpreted in line with the involvement of dorsal object representations in action rather than recognition (Culham & Valyear, 2006; Goodale & Milner, 1992), neurophysiological studies have also shown selectivity for simple shapes (rather than complex objects linked to action processing) in posterior parietal cortex (PPC; Sakata, Tsutsui, & Taira, 2005; Sereno & Maunsell, 1998). Furthermore, neuropsychological studies demonstrate impairments in perceiving global forms after damage to the dorsal visual stream (Riddoch et al., 2008; Shalev, Humphreys, & Mevorach, 2004), suggesting that the dorsal stream plays a necessary role in global form perception. For example, patients with damage to dorsal occipito-parietal cortex have difficulty in perceiving compound global shapes comprising local elements and show a bias to the local forms. Moreover, the ability to perceive the global shape in such cases is linked to activation of the precuneus (Himmelbach, Erb, Klockgether, Moskau, & Karnath, 2009). In addition, damage to PPC can lead to reduced responsivity to global properties of grouped patterns (Han, Jiang, Mao, Humphreys, & Qin, 2005). On the other hand, damage to ventral visual cortex can result in worse identification of parts compared with wholes. For example, patients can be better at identifying silhouettes than line drawings (Riddoch & Humphreys, 1987) and may show a global bias when presented with compound shapes (Riddoch et al., 2008). These findings suggest that global forms are derived in parallel with

[1]University of Birmingham, [2]Bernstein Center for Computational Neuroscience Tübingen, [3]University of Oxford

Journal of Cognitive Neuroscience 26:3, pp. 621–634
doi:10.1162/jocn_a_00489

hierarchical, local-to-global processing, consistent with global form information being used to rapidly access "perceptual hypotheses" about objects in more anterior brain regions (Kveraga, Boshyan, & Bar, 2007). This is also consistent with the role of posterior parietal regions (including the IPS) in discriminating between different types of global Glass patterns (e.g., concentric vs. radial; Li, Mayhew, & Kourtzi, 2009). However, the functional role of these dorsal regions in global pattern processing remains unclear. For example, are regions in the PPC part of a hierarchical pathway of local-to-global processes, or are these regions involved in heterarchical coding, assembling more global representations independently of local form coding, that then influence processing in intermediate visual areas? Also do dorsal regions play a necessary role in global form processing in intermediate ventral regions?

Here, we report a neuropsychological fMRI study that tests for the necessary contribution of higher dorsal visual regions (particularly the IPS) in the processing of global patterns in intermediate areas, such as area V3a and V3b/KO. V3B/KO was defined as the set of contiguous voxels anterior to V3A and inferior to V7 showing significantly higher response to kinetic boundaries than transparent motion (Zeki, Perry, & Bartels, 2003; Dupont et al., 1997).

We measured BOLD activity using fMRI when patients and control participants were presented with Glass patterns (Glass & Perez, 1973; Glass, 1969) to assess the coding of simple visual patterns. These stimuli are ideal for testing global form processing, as different global forms (i.e., concentric, radial, translational patterns) can be derived while the local stimulus statistics across the image are, on average, kept the same and differences in spatial frequency components between the patterns are minimized. In particular, previous behavioral studies have shown that the perception of concentric and radial Glass patterns entails processing of global feature configurations whereas perception of translational patterns entails local orientation processing (Wilson & Wilkinson, 1998; Li & Westheimer, 1997; Olzak & Thomas, 1992). To anticipate, our results show that lesions to the IPS

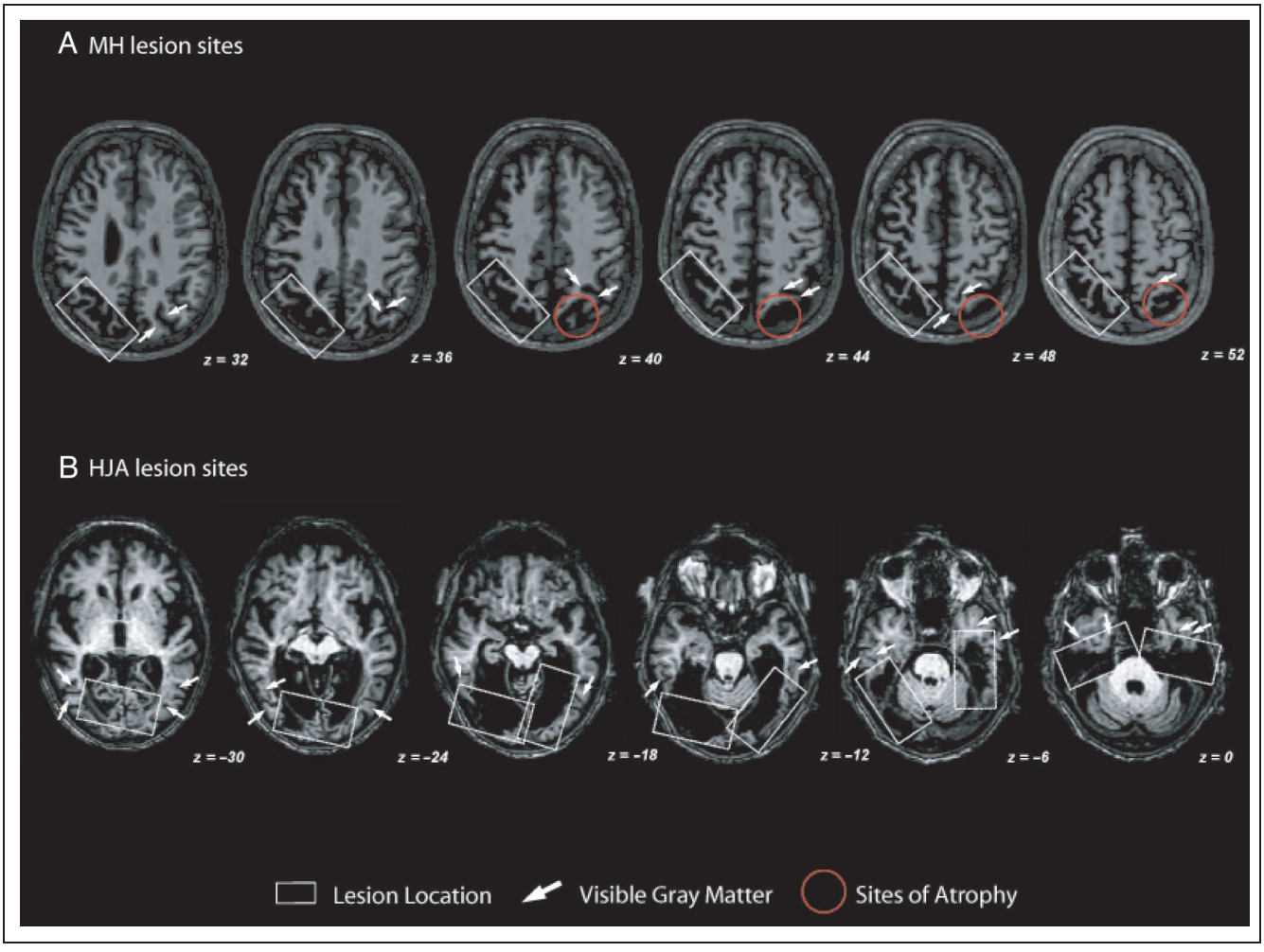

Figure 1. Patient lesion sites. The lesion sites for each patient are shown. The boxes indicate the primary site(s) of damage for both patients. (A) In MH's scan, the circles indicate degenerative change. The white arrows indicate visible gray matter perilesionally for patient HJA and adjacent to the atrophy sites in MH's scan. (B) In HJA's scan, the boxes indicate the lesion sites in both hemispheres.

reduce activity to global radial and concentric patterns in structurally preserved intermediate regions. However, BOLD responses to translational patterns, dependent on local integration processes, are spared. In contrast, damage to ventral cortex leaves the responses to global radial and concentric patterns intact. These results suggest a heterarchical rather than hierarchical account in which independent global integration processes, operating through the PPC, modulate pattern coding in intermediate ventral brain regions.

METHODS

Participants

Two patients and six age-matched controls participated in this study. All participants gave written informed consent and were paid for their participation. The study was approved by the local ethics committee.

Patient MH

MH was a 53 year-old man at the time of testing. He suffered anoxia at the age of 42, which resulted in cortical lesions in bilateral posterior parietal regions (Figure 1A, MH lesion sites), which were more pronounced on the left side (including the occipital-parietal borders, part of the IPS and superior parietal lobe). From a neurological perspective, MH shows extinction under short stimulus presentation conditions (presentations typically under 100 msec) and optic ataxia. MH had intact visual fields on perimetric testing (for details of a clinical assessment, see Rice et al., 2008; Kitadono & Humphreys, 2007; Riddoch et al., 2004). Note that it is unlikely that MH's performance here was affected by extinction given that he showed higher BOLD responses for translational relative to global patterns and that the stimulus duration was at least three times longer than those required to generate extinction in his case.

Patient HJA

HJA was an 86-year-old man when he participated in the experiments. HJA suffered a stroke in 1981 that resulted in damage to the occipital temporal areas from V2 to V4 with some V1 damage affecting the upper visual fields (Figure 1B, HJA lesion sites). HJA was impaired at a number of visual functions including visual object and face recognition, reading, color perception, and navigation. This inability to visually recognize objects, faces, words, and colors and navigate outside a known route has been attributed to a deficit in the perceptual representation of visual stimuli (Riddoch & Humphreys, 1987), although HJA can make use of context and semantic or visual memory efficiently. Also tactile object recognition was spared (see Allen & Humphreys, 2009). Perimetric testing showed a superior altitudinal defect for both visual fields. HJA's case has been reported in detail in Riddoch et al. (1999, 2008) and Riddoch and Humphreys (1987).

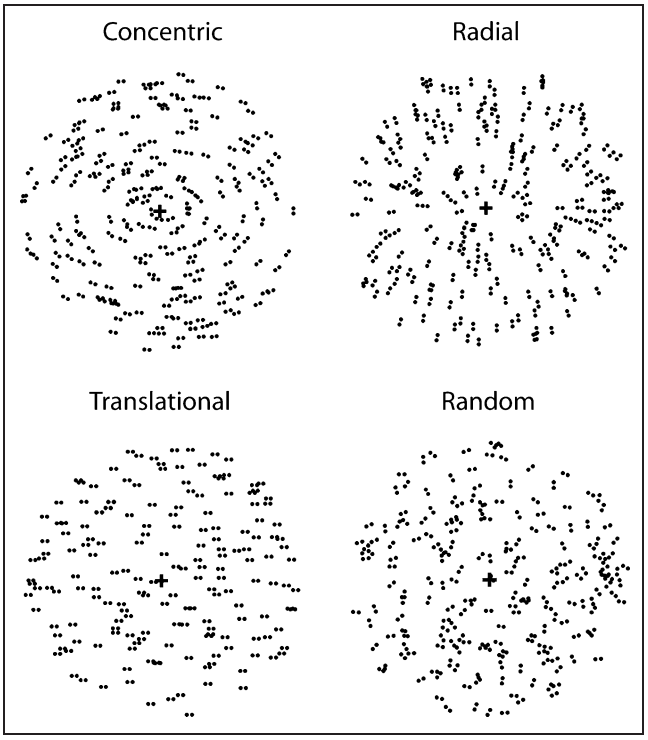

Figure 2. Stimuli. Examples of the different Glass pattern types (concentric, radial, translational) and the random dot dipole patterns used as stimuli.

Controls

We tested three age-matched controls for patient MH (one man and two women, mean age of 58 years at the time of the experiment, range 57–59 years) and three for patient HJA (two men and one woman, mean age of 83 years, range 81–87 years). All controls were healthy volunteers from the West Midlands. We assessed the cognitive function of the control participants in five fields: orientation, registration, attention/calculation, language, and recall using the mini mental test (Folstein, Folstein, & McHugh, 1975). All controls had corrected-to-normal vision and scored within the range of normal cognitive ability (mean = 28.3) and had normal or corrected-to-normal vision and scored 20/20 on a visual acuity test.

Stimuli

Four different stimulus patterns (Glass patterns), defined by dot dipoles, were used in the behavioral and fMRI experiments: concentric, radial, translational, and random (Figure 2). Glass patterns were composed of white dots presented on a black background at 100% contrast, dot density of 0.4%, and Glass shift (distance between dots in

a dipole) of 10 arcmin. All patterns were confined to a circular aperture of 10.8° of visual angle. We generated the concentric and radial Glass patterns by placing dipoles tangentially (concentric stimuli) or orthogonal (radial stimuli) to the circumference of an ellipse (eccentricity = 0.77) centered at the fixation dot. To match the orientations used for the translational Glass patterns, the major axis of the ellipse was oriented between 0° and 180° in steps of 18°, resulting in stimuli for each of the 10 axis orientations. For the random patterns, we assigned a random orientation between 0° and 180° to each dipole (100 random stimuli). Evaluating the distributions of the orientations of the dot dipoles showed similar orientation profiles across all patterns (e.g., mean and standard deviation for concentric: 90.05° ± 51.97°, radial: 90.07° ± 51.97°, translational: 81° ± 54.49°, random: 89.6° ± 51.84°). These parameters were chosen based on previous studies (Ostwald, Lam, Li, & Kourtzi, 2008; Wilson & Wilkinson, 1998). Dot dipoles were generated by creating a pattern of randomly placed dots and then pairing each dot in this seed pattern with a partner dot that was shifted based on a particular geometric rule (Glass & Perez, 1973; Glass, 1969). A new seed pattern was used for each stimulus presented on a trial, resulting in stimuli jittered at the local dipole positions. For the translational Glass patterns, all dipoles were rotated to the same orientation in steps of 18° from 0° to 180°. We manipulated the global structure of the Glass patterns by replacing a percentage of the signal dot pairs by randomly positioned dots. We tested observers' performance in discriminating global Glass patterns from random patterns using constant stimuli presented at different signal levels (percentage of dots that were aligned to a certain global structure). We tested seven (10%, 25%, 40%, 55%, 70%, 85%, 100%) signal levels. Each trial consisted of two sequentially presented stimuli, one random pattern and one Glass pattern. Observers judged which interval contained the Glass pattern. "Catch" trials containing two 100% signal Glass patterns were used to control for the possibility that observers may ignore the second stimulus after detecting a Glass pattern in the first interval. For each pattern, we tested 20–34 trials per signal level. Each stimulus was presented for 332 msec.

Behavioral Measurements

For the behavioral data, we calculated accuracy (percent correct responses) as a function of signal level.

Design

The order of the trials was randomized, and the order of the two stimuli was counterbalanced across trials. The behavioral experiment was self-paced, that is, a new trial would start after the participant's response. Each observer took part in a short practice session before the experiment commenced to become familiar with the patterns, keys, and the task.

Data Analysis

The data were fit by a cumulative Gaussian function using the Psignifit toolbox version 2.5.6 for Matlab (see bootstrap-software.org/psignifit/), which implements the maximum likelihood method described by Wichmann and Hill (2001a, 2001b). The signal percentage thresholds for further statistical analysis were taken to be the 75% correct performance estimated from this fit.

fMRI Measurements

MRI Data Acquisition

The imaging experiments were conducted at the Birmingham University Imaging Centre using a 3T Phillips Achieva scanner. T2*-weighted functional images (2.5 × 2.3 × 3 mm resolution) and T1-weighted anatomical data (1 × 1 × 1 mm resolution) were collected with an eight-channel SENSE head coil. All EPI data (localizer and experimental scans) were acquired from 33 axial slices (2.5 × 2.3 × 3 mm resolution, repetition time = 2000 msec, echo time = 35 msec, flip angle = 80°, field of view = 240 × 96 × 240) that covered the whole brain. Because of the amount required for the completion of all functional scans and the general physical ability of the participants, all data were collected in two to three sessions for each participant.

Design

The same participants who took part in the behavioral experiment participated in the imaging study. Each participant was scanned in one localizer run of the LOC localizer scan and four to six Glass pattern runs. There was a variable number of Glass pattern scans, which depended on the time that the participant could afford to stay in the MR scanner.

LOC Localizer Scans

We localized the LOC using grayscale images of novel and familiar objects as well as scrambled versions of each set (Kourtzi & Kanwisher, 2001). This design resulted in four stimulus conditions: intact familiar, intact novel, scrambled familiar, and scrambled novel. Stimuli were presented in a block design. Each block lasted 16 sec and consisted of 20 stimuli of each condition. Each run consisted of four blocks for each condition and four fixation blocks. The order of all blocks was counterbalanced. Each image was presented for 300 msec followed by 500 msec blank. Observers performed a "1-back matching task," during which they pressed a key to report when two stimuli in a row were the same.

Glass Pattern Experiment Scans

Concentric, radial, translational, and random stimuli were presented in blocks of 16 sec. Concentric, radial, and

translational patterns were presented at 100% signal. Each stimulus was presented for 332 msec followed by a 468-msec fixation interval (trial onset asynchrony, 800 msec). Each observer was scanned on maximum of seven experimental runs. Each run lasted 5.6 min and comprised of the four stimulus conditions (Concentric, Radial, Translational, and Random), four times each in counterbalanced order, and five fixation blocks (one block in the beginning of each run, one in the end, and three interleaved after every set of four experimental blocks). In each block, 20 different stimuli of one type (Concentric, Radial, Translational, and Random) were presented, each with a different random arrangement of dot pairs. Stimuli in each block were randomly sampled twice from the 10 orientations for each stimulus type. That is, 80 of 100 unique stimuli per stimulus type were randomly sampled and presented per run. This design ensured that differences in the fMRI responses across stimulus types could not be attributed to differential adaptation effects related to stimulus repetition. Furthermore, local adaptation across stimuli was controlled and equated across stimulus conditions by generating each stimulus based on a different seed pattern and introducing different global orientation axes across stimuli.

Participants were instructed to fixate on a central fixation dot and press a key when a Glass pattern of higher density compared with the rest of the stimuli appeared

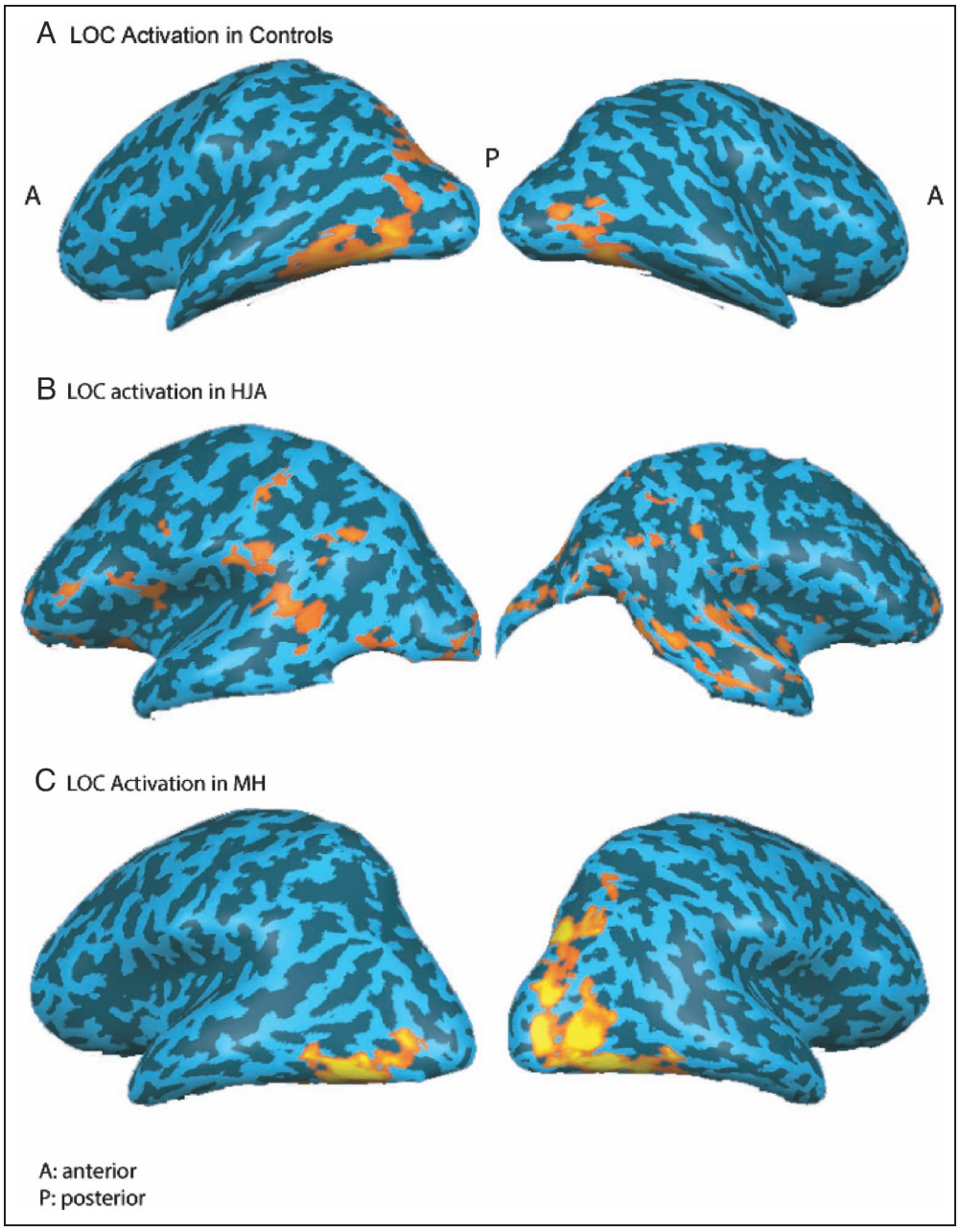

Figure 3. Functional activation maps ($p < .001$) for the contrast of intact versus scrambled images of objects. Activations are shown in the LOC for the control group (A), HJA (B), and MH (C). Activation maps were similar across participants in the control groups, and therefore, the data were pooled across these participants.

on the screen. The same number of these denser stimuli (on average twice per 16 sec block) appeared across conditions and randomly within each block. This task ensured that participants attended to the stimuli, but it did not require recognition of the global patterns that could be difficult for the patients.

fMRI Data Preprocessing

All functional and high-resolution anatomical data were analyzed with Brain Voyager QX (Brain Innovation, Maastricht, The Netherlands). Preprocessing of all functional data included slice-scan time and head movement correction, temporal high-pass filtering (three cycles), and translational trend removal. The anatomical data were transformed into Talairach space (Talairach & Tournoux, 1988) reconstructed in 3-D and inflated. The functional images were aligned to the high-resolution anatomical volume resulting in spatially standardized 4-D volume time-course data.

Mapping ROIs

For each observer, we identified (a) the LOC and (b) regions responding more to concentric and radial Glass patterns than to translational patterns.

We defined the LOC (see Figure 3 for LO activation foci in patients and controls) as the set of contiguous voxels in the ventral occipitotemporal cortex that showed significantly higher responses ($t > 4.0$, $p < .001$) to intact than scrambled images of objects (Kourtzi & Kanwisher, 2000).

General Linear Model Analysis on fMRI Responses to Glass Patterns

To identify regions engaged in the processing of visual forms, we conducted a general linear model (GLM) analysis on gray matter voxels contrasting fMRI responses to Glass patterns with responses to random stimuli. For the group (control participants) analysis, we used smoothed volume time-course data (Gaussian kernel, 6 mm FWHM) modeled with five regressors of interest (four stimulus conditions plus a fixation baseline) convolved with a canonical hemodynamic response function and six additional covariates of interest (the movement parameters obtained during the motion correction for *x*-*y*-*z* translations and rotations). Glass pattern-responsive regions were defined as clusters of activation that showed significantly higher activations for all Glass pattern stimuli compared with random stimuli ($p < .05$, Bonferroni-corrected). For individual participants, we conducted the same GLM analysis ($p < .05$, cluster threshold-corrected) on unsmoothed volumetric time-course data.

Furthermore, we identified cortical regions that responded more strongly to global patterns (concentric and radial Glass patterns) than to translational patterns. We performed GLM analysis across participants (control group analysis) and for individual participants using only gray matter voxels. For the group analysis, smoothed time-course data (Gaussian kernel of 6 mm FWHM) were modeled with five regressors of interest (four stimulus conditions plus fixations baseline condition) convolved with a canonical hemodynamic response function and six covariates of no interest (*x*,*y*,*z* translations and rotations) that were obtained during the motion correction algorithm.

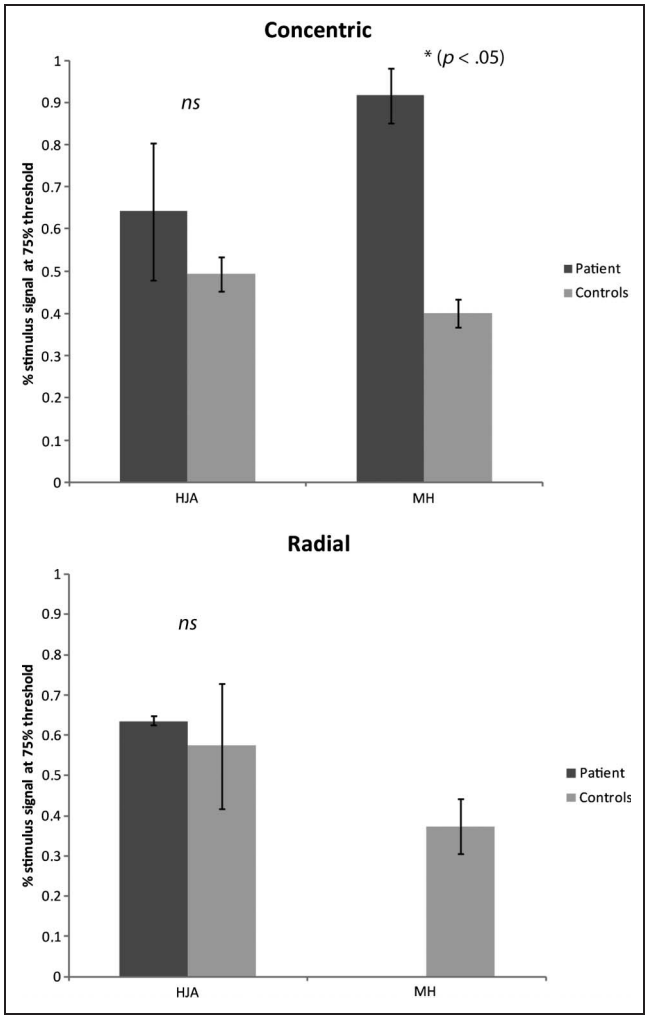

Figure 4. Behavioral results for patients and controls. Data (percent signal at 75% correct performance threshold) is shown for concentric and radial patterns. Note that no data are presented in the case of radial patterns for MH, as performance could not be significantly fit by a cumulative Gaussian function, and therefore, the 75% correct performance threshold could not be correctly calculated. Data for translational patterns are also not shown for patients or controls as both groups of participants were poor in this condition; that is, performance did not reach the 75% correct performance threshold (see Table 1). For the control group, error bars indicate the *SEM* across participants. For patients, error bars indicate the *SEM* across runs (two runs per patient). NS stands for nonsignificant differences between the patients' and controls' performance.

Similar analysis was followed for each individual participant on unsmoothed data.

RESULTS

Behavioral Results

We compared the performance of two patients with lesions respectively in PPC (MH) and occipital-temporal cortex (HJA; Figure 1) with the performance of age-matched controls in the detection of Glass patterns from noise. Observers were presented with two stimulus intervals, one containing a Glass pattern (concentric, radial, or linear) and one containing a random pattern embedded at different noise levels (Figure 2 for stimulus types), and were asked to judge which interval contained the Glass pattern.

Figure 4 compares the performance (% signal dots at 75% correct threshold performance) of controls and patients in Glass pattern detection across signal levels (i.e., number of dot dipoles aligned to the global pattern structure). We fitted the data with a cumulative Gaussian function and calculated 75% correct threshold performance for each participant (see Table 1 for goodness of fit measures and significance values). To assess differences in the processing of Glass patterns between patients and controls, we used a modified F test to compare single cases against a group of participants (Hulleman & Humphreys, 2007). We calculated the mean threshold and variance for each patient and for their respective controls. Our results show that patient HJA, with occipital-temporal lesions affecting areas V1/V2 through to V4, performed similarly to his age-matched controls for global (i.e., concentric, radial) stimulus patterns (concentric: $F(1, 2)_{\text{adjusted}} = 3.41$, $p = .1$; radial: $F(1, 2)_{\text{adjusted}} = 0.04$, $p = .4$). In contrast, MH with posterior parietal lesions showed impaired performance for the detection of radial and concentric patterns compared with his age-matched controls (concentric: $F(1, 1)_{\text{adjusted}} = 80.87$, $p < .05$; for radial patterns, we could not perform statistics on the threshold because MH did not reach 75% threshold performance and the data could not be fit by a reliable function). Finally, consistent with previous findings (Wilson & Wilkinson, 1998), the behavioral results for the control participants showed that translational Glass patterns were poorly detected by both controls and patients and psychometric functions could not be fit (see Table 1). Nevertheless, translational patterns provide an interesting control condition for measuring BOLD activity (see below) related to global (i.e., concentric, radial patterns) versus local processing (i.e., translational patterns; Wilson & Wilkinson, 1998; Li & Westheimer, 1997; Olzak & Thomas, 1992). To ensure that any BOLD differences between global (concentric, radial) and local (translational) Glass patterns were not because of differences in stimulus detectability, we presented all stimuli without noise during scanning.

fMRI Results

To investigate the neural processing of global patterns, we compared activations for global Glass patterns (concentric and radial patterns) with activations for translational patterns (linear) that have been suggested to entail local processing (Wilson & Wilkinson, 1998; Li & Westheimer, 1997; Olzak & Thomas, 1992). GLM analysis of the fMRI data for the control participants (we pooled the data across all control participants as the two control groups showed similar activation patterns) revealed significantly stronger ($p < .05$ cluster threshold-corrected) activations (Figure 5A; see also Table 2) for global than for translational patterns in extrastriate visual areas (including V3a and V3b/KO), the IPS and frontal cortex (medial frontal and superior frontal gyrus). These differences in activation patterns cannot be simply accounted for by differences in the perception of Glass patterns across participants, as participants were tested with Glass patterns presented at 100% signal. When presented without noise, all Glass pattern types were clearly perceived by both controls and patients (as verified by testing in a practice session before scanning). It is important to note that the lower behavioral performance

Table 1. Goodness of Fit Measures

Participants	*75% Threshold*	*R*	*p*
Concentric			
HJA control group	0.4923	0.9818	.0001
HJA	0.6416	0.9357	.0019
MH control group	0.4000	0.9883	.0001
MH	0.9166	0.9194	.0271
Translational			
HJA control group	NaN[a]	0.3978	.3769
HJA	NaN	0.3157	.4903
MH control group	NaN	0.6871	.0881
MH	NaN	0.9886	.0015
Radial			
HJA control group	0.5738	0.9402	.0016
HJA	0.6337	0.8974	.0061
MH control group	0.3742	0.9968	.0001
MH	NaN	0.0636	.9191

Behavioral results for patients and controls. Data (percent signal at 75% correct performance threshold) and goodness of fit measures (R, p values) are shown for concentric, radial, and translational patterns.

[a]NaN indicates that the 75% correct performance threshold could not be correctly calculated either because data were not significantly fit or performance did not reach the 75% correct threshold (e.g., in the case of translational patterns for MH).

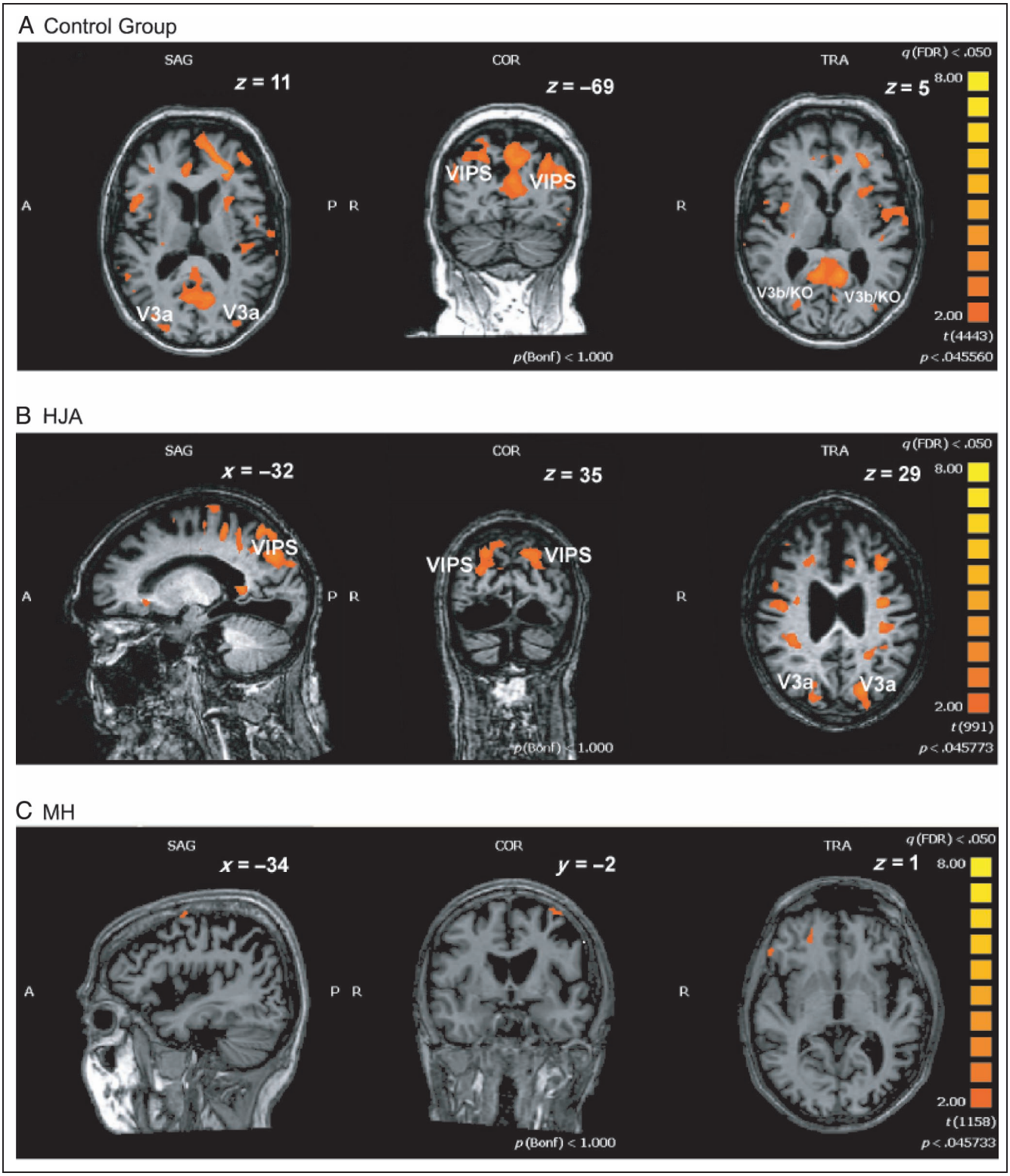

Figure 5. Functional activation maps. Activations ($p < .05$ FDR-corrected) are shown for the contrast of global (concentric + radial) versus local (translational) patterns. Different slices are shown for controls and patients, so that representative activated regions can be shown for each participant group within the space limits of the figure. Tables 2 and 3 show all activated regions including Talairach coordinates for this contrast. Activations in IPS and areas V3a and V3b/KO are shown by relevant labels for (A) the control group (see also Table 2) and (B) HJA (see also Table 3a). (C) Activations for the same contrast are shown for patient MH. Note the lack of significant activations in the IPS, V3a, and V3B/KO (see also Table 3b).

Table 2. Activation Foci for the Contrast Global (C + R) than Translational (T) Patterns (C + R > T) in All Control Participants

	RH			*LH*		
ROI	*X (SD)*	*Y (SD)*	*Z (SD)*	*X (SD)*	*Y (SD)*	*Z (SD)*
Superior frontal gyrus (BA 6)	8 (2.3)	14 (1.8)	63 (1.5)	−14 (3.9)	16 (8.6)	48 (2.9)
Inferior frontal gyrus (BA 47)	29 (2.4)	20 (1.8)	−17 (2.3)	−31 (4.9)	15 (3.2)	−1 (9.5)
Middle frontal gyrus	30 (2.3)	29 (2.4)	25 (2.7)	−9 (2.1)	41 (4.1)	26 (3.6)
Anterior middle frontal gyrus	28 (1.7)	42 (2.1)	22 (1.8)	−36 (3.8)	47 (3.8)	13 (3.6)
Cingulate				−8 (2.5)	−42 (2)	43 (2.3)
Posterior cingulate	7 (3.8)	−51 (4.3)	5 (2.2)	−7 (3.6)	−53 (3.8)	4 (3)
Precentral gyrus (BA 4)	13 (2.1)	−23 (3.3)	72 (1.3)	−2 (2.4)	−34 (3.8)	67 (2.3)
Precentral gyrus (BA 6)	57 (1.7)	−5 (2.2)	30 (2.5)			
Medial pFC				−9 (2.9)	56 (5.1)	17 (3.7)
PMv (BA 46)	37 (3.1)	10 (6.5)	25 (3.6)	−52 (6.7)	−5 (7.4)	3 (4.6)
Insula				−35 (4.8)	−25 (6)	17 (5.4)
Superior temporal gyrus (BA 42)	59 (4.1)	−39 (6.4)	14 (1.9)	−62 (2.2)	−31 (3.3)	19 (3.9)
Intraparietal sulcus (VIPS, POIPS, DIPS)	35 (12)	−55 (14)	42 (7.2)	−35 (6.2)	−68 (3.5)	28 (7.3)
Posterior middle temporal gyrus	41 (1.7)	−67 (1.4)	25 (4.3)			
LO/CoS	37 (3.9)	−53 (4.5)	−13 (3)	−50 (1.8)	−59 (4.3)	−2 (1.3)
PFs				−46 (5.2)	−53 (6.6)	−15 (2.7)
Precuneus	−6 (4.1)	−65 (3.7)	27 (4.5)			
V3b/KO	28 (3.5)	−77 (2.2)	6 (2.6)			
V4v	28 (1.8)	−84 (1.9)	−4 (2.8)			

for the translational patterns was observed only when the stimuli were presented in the context of a detection from noise task.

The same GLM analysis on the data from HJA showed similar activation patterns. We observed significantly stronger ($p < .05$ cluster threshold-corrected) activations for global than translational patterns in anterior temporal areas, the IPS, V3a, and frontal cortex (Figure 5B; see also Table 3a; note that V3b/KO was lesioned in HJA). In contrast, the same GLM analysis on MH's data did not show any significantly higher activations for global than translational patterns in occipital, temporal, or parietal areas (Figure 5C; see also Table 3b). Indeed, we observed higher activation for translational than radial and concentric patterns in a number of regions including V3a and V3b/KO (which were structurally spared in MH; Figure 1). The relatively reduced visual activations for global patterns in MH's visual cortex could not be simply explained by reduced responsiveness of ventral regions to visual stimuli for two reasons. First, activations in intermediate ventral regions were observed for translational stimuli. Second, we observed activations to more complex object stimuli (in an independent localizer scan) in MH's lateral occipital cortex (Figure 3) that were comparable with activations for controls. Dent, Lestou, and Humphreys (2010) have also reported highly significant motion-driven BOLD responses in area hMT+/V5 in this patient, indicating that he generally has a strong BOLD signal. Thus, activation patterns in MH relate to impairments to global compared with local processing rather than overall responsiveness to visual stimuli.

Further support for the above findings comes from analyzing fMRI responses within regions that responded significantly more strongly to Glass patterns than to random stimuli. To assess differences in the processing of global (concentric and radial) and translational patterns between patients and controls, we used the modified F test to compare single cases against a group of participants (Hulleman & Humphreys, 2007), similar to the analysis of psychophysical data. We calculated the mean and variance for each patient, taking into account each run in the Glass pattern experiment (6 for patient HJA and 4 for patient MH). No significant differences were observed between HJA and the controls (Figure 6A and B) in the patterns of activations across all ROIs (MFG: $F(1, 5)_{\text{adjusted}} = 0.05, p = .9$; IPS: $F(1, 3)_{\text{adjusted}} = 0.73, p = .54$; FGs: $F(1, 4)_{\text{adjusted}} = 5.87$, $p = .49$; STG: $F(1, 4)_{\text{adjusted}} = 0.98, p = .75$; V3a: $F(1, 5)_{\text{adjusted}} = 0.07$, $p = .56$). In contrast, we observed significant

differences in V3b/KO, $F(1, 5)_{adjusted} = 18.04, p < .05$, and SFG, $F(1, 4)_{adjusted} = 2.96, p < .05$, for MH compared with the control participants (Figure 6). In particular, MH showed greater activation for translational compared with concentric and radial stimuli, although the controls showed the opposite effect (Figure 6; see also Table 4 for all activation foci and Talairach coordinates for this contrast).

DISCUSSION

Our results provide evidence for the crucial role of PPC in global form perception, suggesting a heterarchical rather than hierarchical model for visual form processing.

Previous studies of hierarchical form coding have largely focused on processing within the ventral visual stream (Ostwald et al., 2008; Wilkinson et al., 2000). For

Table 3. Activation Foci for the Contrast Global (C + R) than Translational (T) Patterns (C + R > T) in Patient HJA and Patient MH

	RH			*LH*		
ROI	*X (SD)*	*Y (SD)*	*Z (SD)*	*X (SD)*	*Y (SD)*	*Z (SD)*
a. Patient HJA						
Superior frontal gyrus	20 (4.1)	17 (5.8)	46 (11)			
Superior frontal gyrus (BA 6)	14 (6.5)	−12 (7.3)	64 (6.7)			
Inferior frontal gyrus (BA 46)	44 (5.6)	42 (4.6)	6 (3.5)	−32 (1.8)	32 (2)	−11 (1.8)
Middle frontal gyrus	47 (1.5)	10 (3.1)	31 (3)			
Anterior middle frontal gyrus (BA 10)	25 (6.5)	54 (4.7)	12 (6.3)	−35 (3.4)	24 (3.9)	26 (3.5)
Precentral gyrus				−16 (4.8)	−23 (4)	67 (3.4)
Postcentral sulcus				−39 (5.7)	−22 (2.8)	29 (6.6)
Premotor dorsal	42 (6.7)	−2.3 (6.6)	26 (13)	−36 (3.3)	−6 (3.6)	46 (7.1)
Cingulate gyrus (BA 32)				−11 (1.8)	26 (2.4)	30 (4.1)
Posterior cingulate (BA 10)	25 (3.2)	−52 (3.7)	10 (3.5)	−25 (3.7)	−50 (3.3)	4 (2.5)
Posterior cingulate	3 (2.6)	−40 (2.4)	38 (2.4)	−6 (24)	−29 (4.8)	45 (5.8)
Insula	33 (3.9)	13 (5.8)	2.2 (6.8)	−33 (3.2)	18 (6.1)	0.19 (7.1)
Posterior insula	37 (6.7)	−32 (4.8)	23 (6.7)			
Medial pFC	8 (2.6)	64 (2.5)	8 (5.4)			
Superior temporal sulcus/gyrus	58 (4.6)	−15 (8.1)	−2 (4.8)	−56 (6)	−35 (12)	0 (7.2)
Middle temporal gyrus	46 (5.3)	−46 (6.7)	−1 (6.1)			
Anterior middle temporal gyrus				−58 (1.9)	1 (2.4)	−11 (2)
Anterior temporal pole				−51 (2.9)	13 (4)	−23 (3.7)
Orbital sulcus				−23 (1.6)	27 (2.1)	−4 (2)
Precuneus	11 (3.9)	−49 (2)	69 (2)			
	3 (2)	−61 (2.9)	33 (2.9)			
Ventral intraparietal area	15 (4.7)	−74 (5.1)	34 (6.7)	−20 (4.3)	−77 (5.9)	30 (4.2)
Parietal occipital intraparietal area	14 (5.1)	−62 (6)	47 (4.5)	−18 (4.7)	−69 (4.1)	46 (3)
Dorsal intraparietal area				−17 (5.2)	−59 (1.7)	51 (2.6)
V3a				−34 (1.7)	−65 (2.6)	34 (2.3)
b. Patient MH						
IFG	51 (2)	33 (2.9)	−3 (2.7)			
MFG	22 (1.3)	43 (2.8)	2 (1.8)			
FEF				−36 (3.7)	−1.8 (3.2)	62 (3.3)

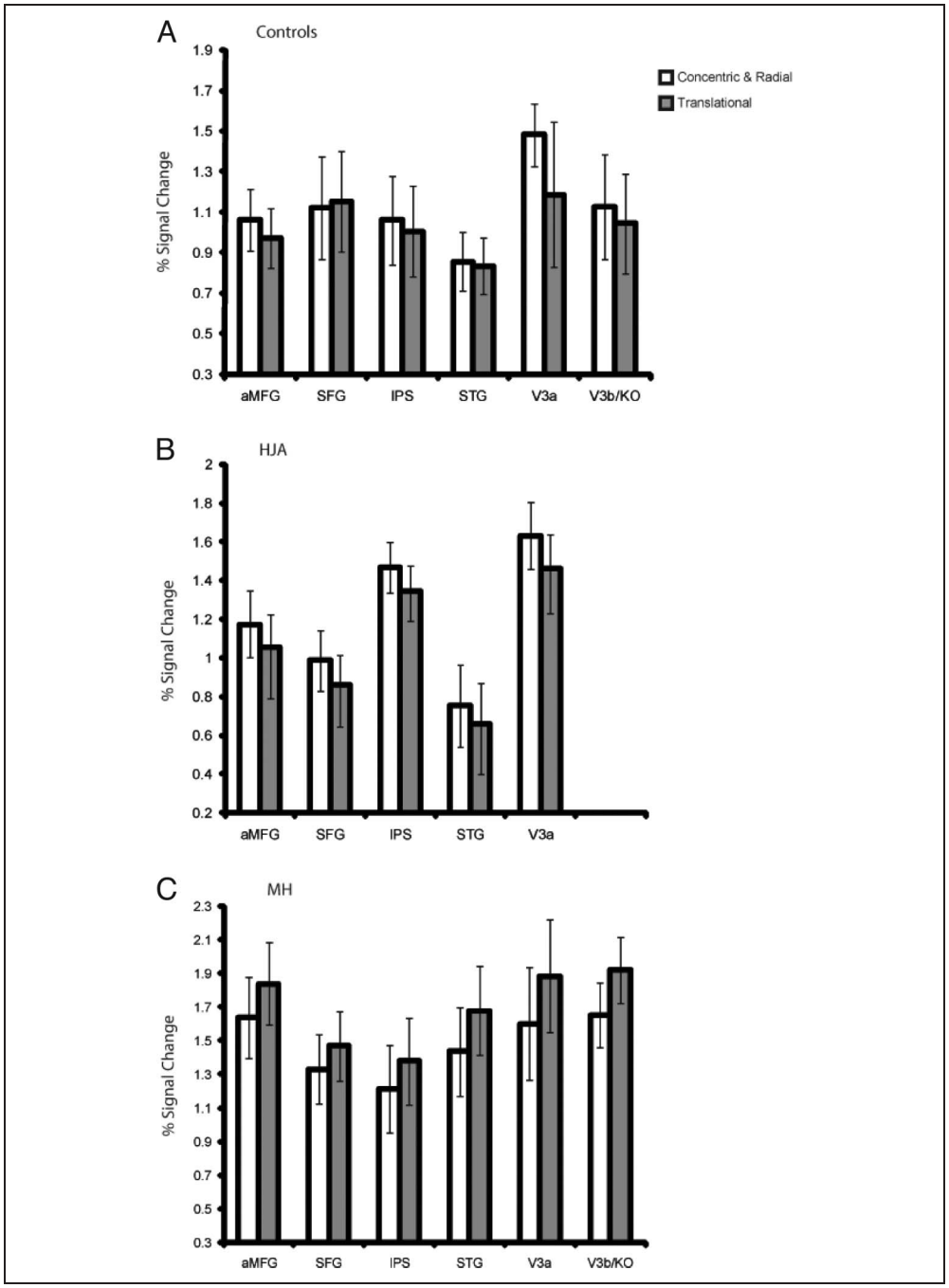

Figure 6. Percent signal change for (A) controls, (B) HJA, and (C) MH for regions that showed significantly stronger activations to all Glass patterns (concentric, radial, translational) versus random dot dipole patterns. Error bars indicate *SEM*. Note that area V3B/KO was lesioned for HJA, and therefore, percent signal change could not be extracted from this area. (aMFG = anterior middle frontal gyrus; SFG = superior frontal gyrus; STG = superior temporal gyrus). See Table 4 for activation foci and Talairach coordinates for controls.

example, previous studies have used Glass patterns (Glass & Perez, 1973; Glass, 1969) to assess processing of visual forms suggesting different mechanisms for local versus global form processing. In particular, translational patterns have been shown to be more difficult to detect from local noise than radial and concentric patterns, suggesting that translational patterns involve local grouping of elements whereas radial and concentric patterns may be coded using more global feature configurations (Wilson & Wilkinson, 1998; Li & Westheimer, 1997; Olzak & Thomas, 1992). Imaging studies have demonstrated that both intermediate and higher-level visual regions are sensitive to Glass patterns whereas early visual regions do not differentiate between organized patterns and randomly oriented elements with matching average local statistics (Li et al., 2009; Ostwald et al., 2008; Chen, Chang, Liu, Chen, & Han, 2004; Wade, Norcia, Vildavski, & Pettet, 2003; Wilkinson et al., 2000). Li et al. (2009) and Ostwald et al. (2008) have further shown that different integration processes can be separated within intermediate visual areas. For example, a region medial to V4 differentiates between Glass patterns and random stimuli but not between different Glass patterns. More dorsal regions corresponding to V3a and V3b/KO differentiate radial and concentric designs from translational

Table 4. Activation Foci for the Contrast of All Glass Patterns versus Random Dot Dipoles in All Controls (CRT > N)

	RH			*LH*		
ROI	*X (SD)*	*Y (SD)*	*Z (SD)*	*X (SD)*	*Y (SD)*	*Z (SD)*
Anterior middle frontal gyrus				−37 (5.8)	44 (7.2)	14 (3.4)
Superior frontal gyrus	29 (4.9)	40 (6.1)	24 (7.4)	−20 (5.7)	38 (11)	12 (4.7)
SFG (BA 10)	17 (2.1)	63 (1.6)	21 (1.7)	−12 (2.1)	17 (2.6)	53 (2.1)
Precentral gyrus (BA 6)	44 (3.7)	−3.7 (2.1)	−23 (0.78)	−54 (2.2)	0.59 (2.2)	23 (2.3)
Premotor dorsal				−35 (4)	−13 (2.5)	40 (5.3)
SEF (medial frontal gyrus)	5 (6.7)	−24 (3.9)	66 (3.9)			
Subgyral (frontal lobe)	26 (3.6)	−2.4 (3)	36 (2.5)			
Insula (BA 10)	46 (3.3)	−34 (4.9)	21 (6.8)			
Insula	47 (1.9)	−13 (1.8)	19 (1.9)			
Intraparietal sulcus (POIPS, DIPS)	11 (4.3)	−79 (3.1)	37 (2.1)	−29 (5.5)	−77 (3.2)	39 (4.5)
				−38 (5.2)	−46 (4.2)	44 (5.2)
Superior temporal gyrus				−42 (6.7)	−34 (6)	18 (2.5)
V3a				−31 (12)	−79 (10)	11 (7.4)
V3b/KO	17 (6.7)	−80 (7.3)	10 (4.9)			
Cingulate (BA 24)	9.5 (3.7)	16 (3.3)	28 (2.7)			
Anterior cingulate	1.1 (5.9)	37 (3)	7.4 (2.8)			
Posterior cingulate	1 (5.7)	−51 (2.8)	3.7 (2.3)			
Parahippocampal gyrus				−24 (4.2)	−16 (1.9)	−17 (2.4)

patterns, indicating sensitivity to more global integration processes. Areas within the LOC and the IPS discriminate between concentric and radial patterns, consistent with grouping elements into specific global configurations (see also Wilkinson et al., 2000). Taken together, these findings support a hierarchical account of form processing based on the progressive integration from local to more global form features, from early visual to intermediate and higher-level areas.

Although these previous imaging studies have been successful in identifying the circuits involved in global form processing, fMRI on its own does not allow us to define the regions critical for global versus local processing. In contrast, combining behavioral and fMRI measurements in neuropsychological patients is useful for addressing this challenge. Using this approach, we propose a heterarchical account of form processing that highlights the critical role of parietal cortex in modulating global form processing in ventral cortex. In particular, by comparing two patients with parietal versus ventral lesions, we show dissociable activation and behavioral performance patterns related to global form processing. That is, parietal lesions resulted in impaired detection of global forms and a lack of significant activation for global compared with local forms in ventral visual areas, whereas ventral lesions resulted in spared detection performance for global forms that was comparable to the performance of control participants.

Specifically, MH has spared early and intermediate visual areas and a lesion affecting more superior dorsal areas around the IPS. Relative to controls and HJA (the ventral-lesioned patient), MH's behavioral performance was impaired for radial and concentric forms. Activations for translational patterns were evident in brain areas, including the frontal gyrus and V3b/KO, which were intact in MH and reliably activated by global forms for the other participants. This lack of significant activation for global radial and concentric forms cannot be simply attributed to generalized low fMRI responses in this patient given the frontal and V3b/KO activations for translational patterns and also that previous studies have shown strong and reliable activation in MH's ventral cortex (Dent et al., 2010; see also Supplementary Figure 1). Frontal cortex areas have been shown to play a role in the categorization of Glass patterns (Li et al., 2009; Ostwald et al., 2008). The intermediate dorsal region V3b/KO may be thought to form locally based integration of global patterns feeding forward to higher-level regions. However, the lack of global sensitivity to radial and concentric patterns in this structurally spared ventral region in MH indicates that global processing in ventral cortex is contingent on IPS regions that are lesioned in his case. Thus, our findings suggest that the

IPS, previously identified in fMRI studies (Li et al., 2009), plays a causal role in global form processing and potentially modulates processing in intermediate ventral regions (V3b/KO). This is consistent with prior EEG findings showing that early visual-evoked responses to global Gestalt patterns (rows and columns of visual elements) are disrupted by damage to the PPC (Han & Humphreys, 2007). Patients with PPC lesions are also typically impaired at identifying global compound shapes in contrast to the identification of local shapes that remains spared (e.g., Riddoch et al., 2010). Furthermore, our findings are consistent with the role of parietal cortex in spatial attention and the detection of salient stimuli in clutter that may in turn modulate processing in visual cortex (Mevorach, Hodsoll, Allen, Shalev, & Humphreys, 2010; Corbetta & Shulman, 2002; Gottlieb, Kusunoki, & Goldberg, 1998).

Finally, patient HJA with occipitotemporal lesions had similar behavioral and fMRI activation patterns for global radial and concentric form patterns to age-matched control participants. This indicates that extensive damage to ventral extrastriate cortex is not sufficient to disrupt the processing of global radial and concentric Glass patterns. Given that these patterns cannot be distinguished from translational patterns from their spatial frequency components or their average local orientation statistics, these results support the case for global integration processes, which operate independent of the ventral visual regions damaged in HJA's case. This fits with previous reports showing that HJA has intact responses to global compound forms, which may also be coded through more dorsal visual regions (Riddoch et al., 2008; Humphreys, Riddoch, & Quinlan, 1985), and also that he maintains an ability to average across oriented elements (Allen, Humphreys, & Bridge, 2007). Prior studies on HJA have also indicated sensitivity to collinear elements, consistent with his responses to Glass patterns here, but poor subsequent assembly of the grouped segments into multipart objects (Giersch, Humphreys, Boucart, & Kovacs, 2000). This result suggests that global integration processes as studied here are not sufficient for normal object recognition, as the resultant object descriptions may lack the local detail to help code and differentiate multipart objects. The recognition of individual objects can be impaired when local integration processes are disrupted, as is the case for HJA.

The generality of our results with other types of stimuli remains to be tested. Although our study did not test other stimuli related to local–global pattern processing, previous psychophysical studies have shown similar effects on local–global pattern processing using different stimuli (e.g., radial frequency patterns; Habak, Wilkinson, Zakher, & Wilson, 2004; Wilkinson, Wilson, & Habak, 1998). Brain imaging studies on local–global tasks using other types of stimuli (Navon figures (Navon, 1977), parametrically degraded objects, etc.) also implicate the parietal cortex in global form processing (Huberle & Karnath, 2012; Fink, Marshall, Halligan, & Dolan, 1999; Fink et al., 1997; Rafal, 1997) and suggest that disruption of function in parietal areas results in impaired global form perception (Himmelbach et al., 2009; Han et al., 2005). In future studies, it will be interesting to test patients and compare the brain circuits involved in the processing of different stimulus sets manipulating local–global processing.

In summary, our findings propose a heterarchical account for global pattern processing that can be implemented by more than one form of computation: local feed-forward processes operate in parallel with a global integration process that feeds back to modulate intermediate processing. We suggest that complete visual recognition may depend on bringing together local feed-forward processes with the broad description derived from the independent, dorsally mediated, more global processing of shape, to provide full differentiation between objects (see Riddoch et al., 2008).

Acknowledgments

We would like to thank Matthew Dexter for help with data analysis tools. This work was supported by grants from the BBSRC (BB/D52199X/1, BB/E027436/1) and the European Community's Seventh Framework Programme FP7/2007-2013 under Grant Agreement 214728 to Z. K. and the Medical Research Council, Leverhulme Trust and Stroke Association to G. W. H.

Reprint requests should be sent to Dr. Vaia Lestou, School of Psychology, University of Birmingham, Edgbaston, B15 2TT, United Kingdom, or via e-mail: v.lestou@bham.ac.uk.

REFERENCES

Allen, H. A., & Humphreys, G. W. (2009). Direct tactile stimulation of dorsal occipito-temporal cortex in a visual agnosic. *Current Biology, 19,* 1044–1049.

Allen, H. A., Humphreys, G. W., & Bridge, H. (2007). Ventral extrastriate cortical areas are required for optimal orientation averaging. *Vision Research, 47,* 766–775.

Chen, C.-C., Chang, H.-C., Liu, C.-L., Chen, C.-F., & Han, H.-Y. (2004). The human brain responses to Glass patterns: The effects of signal to noise ratio. *Journal of Vision, 4,* 714.

Corbetta, M., & Shulman, G. L. (2002). Control of goal-directed and stimulus-driven attention in the brain. *Nature Reviews Neuroscience, 3,* 201–215.

Culham, J. C., & Valyear, K. F. (2006). Human parietal cortex in action. *Current Opinion in Neurobiology, 16,* 205–212.

Dent, K., Lestou, V., & Humphreys, G. W. (2010). Deficits in visual search for conjunctions of motion and form after parietal damage but with spared hMT+/VS. *Cognition of Neuropsychology, 27,* 72–99.

Dupont, P., De Bruyn, B., Vandenberghe, R., Rosier, A. M., Michiels, J., Marchal, G., et al. (1997). The kinetic occipital region in human visual cortex. *Cerebral Cortex, 7,* 283–292.

Fink, G. R., Halligan, P. W., Marshall, J. C., Frith, C. D., Frackowiak, R. S., & Dolan, R. J. (1997). Neural mechanisms involved in the processing of global and local aspects of hierarchically organized visual stimuli. *Brain, 120,* 1779–1791.

Fink, G. R., Marshall, J. C., Halligan, P. W., & Dolan, R. J. (1999). Hemispheric asymmetries in global/local processing are modulated by perceptual salience. *Neuropsychologia, 37,* 31–40.

Folstein, M. F., Folstein, S. E., & McHugh, P. R. (1975). "Mini-mental state". A practical method for grading the cognitive

state of patients for the clinician. *Journal of Psychiatric Research, 12,* 189–198.
Giersch, A. (2002). Modulations of the processing of line discontinuities under selective attention conditions? *Perception & Psychophysics, 64,* 67–88.
Giersch, A., Humphreys, G. W., Boucart, M., & Kovacs, I. (2000). The computation of occluded contours in visual agnosia: Evidence for early computation prior to shape binding and figure-ground coding. *Cognition of Neuropsychology, 17*.
Glass, L. (1969). Moire effect from random dots. *Nature, 223,* 578–580.
Glass, L., & Perez, R. (1973). Perception of random dot interference patterns. *Nature, 246,* 360–362.
Goodale, M. A., & Milner, A. D. (1992). Separate visual pathways for perception and action. *Trends in Neurosciences, 15,* 20–25.
Gottlieb, J. P., Kusunoki, M., & Goldberg, M. E. (1998). The representation of visual salience in monkey parietal cortex. *Nature, 391,* 481–484.
Habak, C., Wilkinson, F., Zakher, B., & Wilson, H. R. (2004). Curvature population coding for complex shapes in human vision. *Vision Research, 44,* 2815–2823.
Han, S., & Humphreys, G. W. (2007). The fronto-parietal network and top–down modulation of perceptual grouping. *Neurocase, 13,* 278–289.
Han, S., Jiang, Y., Mao, L., Humphreys, G. W., & Qin, J. (2005). Attentional modulation of perceptual grouping in human visual cortex: ERP studies. *Human Brain Mapping, 26,* 199–209.
Himmelbach, M., Erb, M., Klockgether, T., Moskau, S., & Karnath, H. O. (2009). fMRI of global visual perception in simultanagnosia. *Neuropsychologia, 47,* 1173–1177.
Huberle, E., & Karnath, H. O. (2012). The role of temporo-parietal junction (TPJ) in global Gestalt perception. *Brain Structure & Function, 217,* 735–746.
Hulleman, J., & Humphreys, G. W. (2007). Maximizing the power of comparing single cases against a control sample: An argument, a program for making comparisons, and a worked example from the Pyramids and Palm Trees Test. *Cognitive Neuropsychology, 24,* 279–291.
Humphreys, G. W., Riddoch, M. J., & Quinlan, P. T. (1985). Interactive processes in perceptual organization: Evidence from visual agnosia. In M. I. Posner & O. S. Marin (Eds.), *Attention and performance XI* (pp. 301–319). Hillsdale, NJ: Erlbaum.
Kitadono, K., & Humphreys, G. W. (2007). Interactions between perception and action programming: Evidence from visual extinction and optic ataxia. *Cognition of Neuropsychology, 24,* 731–754.
Konen, C. S., & Kastner, S. (2008). Two hierarchically organized neural systems for object information in human visual cortex. *Nature Neuroscience, 11,* 224–231.
Kourtzi, Z., & Kanwisher, N. (2000). Cortical regions involved in perceiving object shape. *Journal of Neuroscience, 20,* 3310–3318.
Kourtzi, Z., & Kanwisher, N. (2001). Representation of perceived object shape by the human lateral occipital complex. *Science, 293,* 1506–1509.
Kveraga, K., Boshyan, J., & Bar, M. (2007). Magnocellular projections as the trigger of top–down facilitation in recognition. *Journal of Neuroscience, 27,* 13232–13240.
Li, S., Mayhew, S. D., & Kourtzi, Z. (2009). Learning shapes the representation of behavioral choice in the human brain. *Neuron, 62,* 441–452.
Li, W., & Westheimer, G. (1997). Human discrimination of the implicit orientation of simple symmetrical patterns. *Vision Research, 37,* 565–572.
Mevorach, C., Hodsoll, J., Allen, H., Shalev, L., & Humphreys, G. (2010). Ignoring the elephant in the room: A neural circuit to downregulate salience. *Journal of Neuroscience, 30,* 6072–6079.
Milner, A. D., Perrett, D. I., Johnston, R. S., Benson, P. J., Jordan, T. R., Heeley, D. W., et al. (1991). Perception and action in "visual form agnosia". *Brain, 114,* 405–428.
Navon, D. (1977). Forest before trees: The precedence of global features in visual perception. *Cognitive Psychology, 9,* 353–383.
Olzak, L. A., & Thomas, J. P. (1992). Configural effects constrain Fourier models of pattern discrimination. *Vision Research, 32,* 1885–1898.
Ostwald, D., Lam, J. M., Li, S., & Kourtzi, Z. (2008). Neural coding of global form in the human visual cortex. *Journal of Neurophysiology, 99,* 2456–2469.
Rafal, R. D. (1997). Balint syndrome. In T. E. Feinberg & M. J. Farah (Eds.), *Behavioral neurology and neuropsychology* (pp. 337–356). New York: McGraw-Hill.
Rice, N. J., Edwards, M. G., Schindler, I., Punt, T. D., McIntosh, R. D., et al. (2008). Delay abolishes the obstacle avoidance deficit in unilateral optic ataxia. *Neuropsychologia, 46,* 1549–1557.
Riddoch, M. J., Chechlacz, M., Mevorach, C., Mavntsaki, E., Allen, H., & Humphreys, G. W. (2010). The neural mechanisms of visual selection, the view from neuropsychology. *Annals of the New York Academy of Sciences, 1191,* 156–181, 731–759.
Riddoch, M. J., & Humphreys, G. W. (1987). A case of integrative visual agnosia. *Brain, 110,* 1431–1462.
Riddoch, M. J., Humphreys, G. W., Akhtar, N., Allen, H., Bracewell, R. M., & Schofield, A. J. (2008). A tale of two agnosias: Distinctions between form and integrative agnosia. *Cognitive Neuropsychology, 25,* 56–92.
Riddoch, M. J., Humphreys, G. W., Gannon, T., Blott, W., & Jones, V. (1999). Memories are made of this: The effects of time on stored visual knowledge in a case of visual agnosia. *Brain, 122,* 537–559.
Riddoch, M. J., Humphreys, G. W., Jacobson, S., Pluck, G., Bateman, A., & Edwards, M. (2004). Impaired orientation discrimination and localisation following parietal damage: On the interplay between dorsal and ventral processes in visual perception. *Cognitive Neuropsychology, 21,* 597–623.
Sakata, H., Tsutsui, K., & Taira, M. (2005). Toward an understanding of the neural processing for 3D shape perception. *Neuropsychologia, 43,* 151–161.
Sereno, A. B., & Maunsell, J. H. (1998). Shape selectivity in primate lateral intraparietal cortex. *Nature, 395,* 500–503.
Shalev, L., Humphreys, G. W., & Mevorach, C. (2004). Global processing of compound letters in a patient with Balint's syndrome( ). *Cognitive Neuropsychology, 22,* 737–751.
Talairach, J., & Tournoux, P. (1988). *Co-planar stereotaxic atlas of the human brain: 3-Dimensional proportional system—An approach to cerebral imaging*. New York: Thieme.
Wade, A., Norcia, A., Vildavski, V., & Pettet, M. (2003). fMRI of Glass patterns. *Journal of Vision, 3,* 50.
Wichmann, F. A., & Hill, N. J. (2001a). The psychometric function: I. Fitting, sampling, and goodness of fit. *Perception & Psychophysics, 63,* 1293–1313.
Wichmann, F. A., & Hill, N. J. (2001b). The psychometric function: II. Bootstrap-based confidence intervals and sampling. *Perception & Psychophysics, 63,* 1314–1329.
Wilkinson, F., James, T. W., Wilson, H. R., Gati, J. S., Menon, R. S., & Goodale, M. A. (2000). An fMRI study of the selective activation of human extrastriate form vision areas by radial and concentric gratings. *Current Biology, 10,* 1455–1458.
Wilkinson, F., Wilson, H. R., & Habak, C. (1998). Detection and recognition of radial frequency patterns. *Vision Research, 38,* 3555–3568.
Wilson, H. R., & Wilkinson, F. (1998). Detection of global structure in Glass patterns: Implications for form vision. *Vision Research, 38,* 2933–2947.
Zeki, S., Perry, R. J., & Bartels, A. (2003). The processing of kinetic contours in the brain. *Cerebral Cortex, 13,* 189–202.